A model for the viscous dissipation rate in stably stratified, sheared turbulence

H. E. Fossum,[1,2,3] E. M. M. Wingstedt,[1,2] and B. A. P. Reif[1,2,4]

Received 8 May 2013; revised 11 June 2013; accepted 13 June 2013; published 19 July 2013.

[1] A model for the turbulence dissipation rate in stably stratified shear turbulence is developed and validated. The functional dependence of the model is derived from first principles and it represents a conceptually new approach in that it depends on the background temperature field rather than on the fluctuating velocity field. This novel feature makes the proposed model a viable candidate for dissipation rate estimates in measured real-life flows. Direct numerical simulation data are used for a priori assessment of the proposed model. It is demonstrated that the proposed model performs very well, particularly in cases where the background stratification becomes dynamically important. Also, a generalized expression for the mixing coefficient has been rigorously derived from first principles assuming local isotropy of incompressible turbulent flows. The mixing coefficient is shown to depend on the Prandtl number and values are in correspondence with previous studies.
Citation: Fossum, H. E., E. M. M. Wingstedt, and B. A. P. Reif (2013), A model for the viscous dissipation rate in stably stratified, sheared turbulence, *Geophys. Res. Lett.*, *40*, 3744–3749, doi:10.1002/grl.50663.

1. Introduction

[2] The viscous dissipation rate of turbulence kinetic energy, ε, is an important property of turbulent flows. It physically represents the conversion of kinetic energy into thermal energy due to viscous forces. The dissipation rate of turbulence kinetic energy is frequently used to characterize the dynamics of turbulence, e.g., in connection with energy transfer across the inertial subrange and for length and time scale characterization of the flow.

[3] Atmospheric flows are usually affected by stratification due to temperature variations, which significantly alters the intensity and structure of the flow field. In stably stratified flows, the buoyancy force tends to reduce turbulence intensities and the associated mixing, whereas in unstable flows, buoyancy acts to enhance turbulence by increasing the vertical momentum exchange.

[4] Because of the directional preference of buoyancy, it is clear that the energetic scales of motion in a stratified, turbulent flow are anisotropic. Ever since *Kolmogorov* [1941], it has been argued that, at least for high Reynolds numbers, directional information is lost as energy propagates from the large to the small scales of turbulence across the inertial subrange. Hence, anisotropy on the large scales will not result in small-scale anisotropy. However, for the last decades, evidence against this belief has grown steadily, as discussed in more detail by, e.g., *Wyngaard* [2010, p. 319].

[5] In the context of stratified shear flow, many authors [e.g., *Yamazaki and Osborn*, 1990; *Thoroddsen and Van Atta*, 1992; *Smyth and Moum*, 2000] currently hold the view that there exists a certain buoyancy Reynolds number, defined as $\mathrm{Re_b} = \varepsilon/\nu N^2$, where N is the Brunt-Väisälä frequency, below which some degree of anisotropy prevails even at the dissipative scales. *Reif and Andreassen* [2003] have theoretically shown that the concept of local isotropy is formally inconsistent with the Navier-Stokes equations in homogeneously sheared turbulent flows affected by stable stratification.

[6] In the laboratory setups and atmospheric field trials, measurements of fluctuating velocity gradients are limited to a few components only. Direct access to the dissipation rate is therefore only available in direct numerical simulations (DNS) of canonical flow problems. Although the DNS approach is limited to fairly low Reynolds numbers, it nevertheless has become a very valuable research tool in order to elucidate the physical characteristics of turbulent fluid motion. In order to provide reasonable estimates of the rate of viscous dissipation in real-life flows, empirical models based on measurable quantities are therefore needed.

[7] Dissipation rate models can be grouped into two different categories; algebraic and integral models. The latter kind of estimates are based on, for instance, spectra or structure functions [e.g., *Limbacher*, 2010; *Xu and Chen*, 2012]. The present study is concerned with the former class of models.

[8] One of the most commonly used algebraic formulas is based on the assumption of isotropic turbulence [*Taylor*, 1935]. This enables the dissipation rate to be computed using only one (out of nine) velocity gradient correlations. One inherent limitation of these models is, however, that they do not depend on the temperature field which becomes dynamically important in stratified turbulence.

[9] As a consequence of the anisotropic nature of stratified turbulence, *Thoroddsen and Van Atta* [1992] suggested that more refined dissipation rate estimates should utilize the Brunt-Väisälä frequency in order to account for stratification. Crude estimates of this kind had already been discussed by *Weinstock* [1981]. Another way of implicitly allowing for stratification is to adopt the assumption of local axisymmetry [*Batchelor*, 1946], which is the basis for models such as that by *George and Hussein* [1991]. Although these models are based on a sound physical basis, they require too

[1]Norwegian Defence Research Establishment (FFI), Kjeller, Norway.
[2]Department of Mathematics, University of Oslo, Blindern, Oslo, Norway.
[3]Nammo Raufoss AS, Raufoss, Norway.
[4]UNIK, Kjeller, Norway.

Corresponding author: H. E. Fossum, Norwegian Defence Research Establishment (FFI), PO Box 25, NO-2027 Kjeller, Norway. (hannibal.fossum@ffi.no)

0094-8276/13/10.1002/grl.50663

many components of the dissipation rate, i.e., $\langle \partial_k u_i \partial_k u_i \rangle$, to be measured, which makes these models a less desirable choice in real-life flows.

[10] A DNS of a Kelvin-Helmholtz instability in a stably stratified flow was reported by *Werne et al.* [2005]. This statistically unsteady flow simulation provides turbulence statistics which can be used to calculate both dissipation rate estimates and the true value of the dissipation rate. In the present paper, a new model for the dissipation rate in a stably stratified environment is proposed and compared to two existing algebraic turbulence dissipation rate models, and the DNS data of *Werne et al.* [2005].

2. Mathematical Modeling

2.1. Fundamental Equations

[11] The present analysis is based on the dynamical equations governing single-point correlations in sheared turbulent flows of an incompressible Newtonian fluid. The Boussinesq approximation is invoked to account for the imposition of density stratification. The equations governing conservation of mass, momentum, and energy are given by

$$\partial_i \tilde{u}_i(\boldsymbol{x},t) = 0, \tag{1}$$

$$\partial_t \tilde{u}_i(\boldsymbol{x},t) + \tilde{u}_j(\boldsymbol{x},t)\partial_j \tilde{u}_i(\boldsymbol{x},t) = -\frac{\partial_i \tilde{p}(\boldsymbol{x},t)}{\rho_0} + \nu \partial_j \partial_j \tilde{u}_i(\boldsymbol{x},t) + \frac{\rho(\boldsymbol{x},t)}{\rho_0} g_i, \tag{2}$$

$$\partial_t \tilde{\theta}(\boldsymbol{x},t) + \tilde{u}_j(\boldsymbol{x},t)\partial_j \tilde{\theta}(\boldsymbol{x},t) = \kappa \partial_j \partial_j \tilde{\theta}(\boldsymbol{x},t) + 2\frac{\nu}{c_v}\tilde{s}_{ij}(\boldsymbol{x},t)\tilde{s}_{ij}(\boldsymbol{x},t), \tag{3}$$

where Einstein's summation convention has been used. Here $\tilde{u}_i(\boldsymbol{x},t)$, $\tilde{p}_i(\boldsymbol{x},t)$, and $\tilde{\theta}(\boldsymbol{x},t)$ denote the instantaneous velocity, pressure, and temperature fields, respectively. ρ_0 is a constant reference density, and $\tilde{s}_{ij} = \frac{1}{2}(\partial_j \tilde{u}_i(\boldsymbol{x},t) + \partial_i \tilde{u}_j(\boldsymbol{x},t))$ is the instantaneous rate-of-strain tensor. Spatial and temporal differentiation are denoted $\partial_i = \partial/\partial x_i$ and $\partial_t = \partial/\partial t$, respectively. Gravitational acceleration in the x_i direction is g_i, whereas ν, κ, and c_v represent the kinematic viscosity, thermal diffusivity, and specific heat capacity, respectively. The Boussinesq approximation reads $\rho(\boldsymbol{x},t)/\rho_0 = (1 - \beta(\tilde{\theta}(\boldsymbol{x},t) - \Theta_0))$, where $\beta = 1/\Theta_0$ defines the thermal expansion coefficient, and Θ_0 is a reference temperature. $\boldsymbol{x} = [x_1, x_2, x_3]$ and t refer to spatial and temporal coordinates, respectively.

[12] The dependent variables ($\tilde{u}_i$, $\tilde{p}_i$, and $\tilde{\theta}$) can without loss of generality be decomposed into a mean and a fluctuating part, e.g., for the velocity field, $\tilde{u}_i(\boldsymbol{x},t) = U_i(\boldsymbol{x},t) + u_i(\boldsymbol{x},t)$. Here $U_i(\boldsymbol{x},t) = \langle \tilde{u}_i(\boldsymbol{x},t) \rangle$ denotes the ensemble averaged velocity, whereas $u_i(\boldsymbol{x},t)$ is the corresponding fluctuating field.

[13] By utilizing this decomposition, the equation governing the dissipation rate $\varepsilon_{i\theta}(\boldsymbol{x},t) = (\kappa+\nu)\langle \partial_j \theta \partial_j u_i \rangle$ of turbulent heat flux, $\langle u_i \theta \rangle$, can now be rigorously derived from (1)–(3). The result can be written as

$$\begin{aligned}\partial_t \varepsilon_{i\theta} + U_k \partial_k \varepsilon_{i\theta} &= -\varepsilon_{k\theta}\partial_k U_i - 2\langle \partial_m \theta \partial_k u_i \rangle \partial_m U_k \\ &+ 4\frac{\nu}{c_v}\langle \partial_m u_i \partial_m s_{kj} \rangle S_{kj} \\ &+ (\kappa+\nu)[\langle u_k \partial_m \theta \rangle \partial_k \partial_m U_i + \langle u_k \partial_m u_i \rangle \partial_k \partial_m \Theta] \\ &- \frac{1+Pr}{2}\left[\frac{1}{\mathrm{Pr}}\varepsilon_{ik}\partial_k \Theta + \beta g_i \varepsilon_\theta\right] + \mathcal{F}_{i\theta},\end{aligned} \tag{4}$$

where the independent variables are omitted for simplicity. Here $s_{kj}(\boldsymbol{x},t)$ and $S_{kj}(\boldsymbol{x},t)$ denote the fluctuating and averaged rate-of-strain tensors, respectively. $\mathrm{Pr} = \nu/\kappa$ is the molecular Prandtl number, $\mathcal{F}_{i\theta}(\boldsymbol{x},t)$ represents correlations of higher-order derivatives of the fluctuating velocity and temperature fields, and $\varepsilon_{ij}(\boldsymbol{x},t) = 2\nu\langle \partial_k u_i \partial_k u_j \rangle$ is the viscous dissipation rate tensor [cf. *Reif and Andreassen*, 2003]. Contraction of $\varepsilon_{ij}(\boldsymbol{x},t)$ yields twice the viscous dissipation rate of turbulence kinetic energy, i.e., $\varepsilon = \frac{1}{2}\varepsilon_{ii}$. The thermal dissipation rate is given by $\varepsilon_\theta = 2\kappa\langle \partial_i \theta \partial_i \theta \rangle$.

2.2. Dissipation Rate Modeling

2.2.1. Locally Isotropic Limit

[14] In the limit of isotropic turbulence, all statistical correlations of the fluctuating velocity and temperature fields must display invariance to arbitrary reflections and rotations. For any given order, a general isotropic tensor can be written as a linear combination of a set of linearly independent isotropic tensors. The number of isotropic tensors depends on the order of the tensor itself. Following *Reif and Andreassen* [2003], the isotropic limit of (4), which comprises tensors up to the third order, is obtained by noting that the most general isotropic form of any first, second, or third-order tensor can be written as

$$\begin{aligned}\mathcal{X}_i &= 0, \\ \mathcal{X}_{ij} &= \gamma_2 \delta_{ij} = \frac{1}{3}\mathcal{X}_{mm}\delta_{ij}, \\ \mathcal{X}_{ijk} &= \gamma_3 \epsilon_{ijk} = 0,\end{aligned} \tag{5}$$

where γ_i are scalars, δ_{ij} is the Kronecker delta, and ϵ_{ijk} is the Levi-Civita alternating tensor. Hence, in the limit of isotropic turbulence only tensors of orders zero and two will remain in (4). Imposing the isotropy constraint, (5), on (4) yields

$$\frac{2}{3}\kappa \partial_m \langle u_m \theta \rangle \partial_k \partial_k U_i = \frac{2}{3}\mathrm{Pr}^{-1}\varepsilon \partial_i \Theta + \beta g_i \varepsilon_\theta. \tag{6}$$

[15] This physically implies that if the turbulence would be truly isotropic, $\varepsilon(\boldsymbol{x},t)$ should be exactly balanced according to (6). As pointed out by *Reif and Andreassen* [2003], it is unlikely that this relation would hold exactly, making the assumption of local isotropy approximative.

2.2.2. Generalized Mixing Efficiency

[16] The mixing efficiency coefficient, Γ, is used to predict small-scale mixing processes in atmospheric science and oceanography. It is defined as the ratio of dissipation of available potential energy to dissipation of turbulence kinetic energy, i.e., $\Gamma = \varepsilon_p/\varepsilon$, where $\varepsilon_p = (\beta g/N)^2 \varepsilon_\theta$. Using this definition, (6) can thus be written as

$$\Gamma = \frac{\varepsilon_p}{\varepsilon} = \frac{2}{3}\mathrm{Pr}^{-1} - \frac{2\kappa \partial_m \langle u_m \theta \rangle \partial_k \partial_k U_i}{3\varepsilon \partial_i \Theta}, \tag{7}$$

which is valid for an incompressible fluid in the limit of locally isotropic turbulence. Previous studies have shown values of Γ in the range between 0.33 and 1 for atmospheric flows [*Galperin and Sukoriansky*, 2010]. However, *McIntyre* [1989] reports that Γ might not be constant, but can vary by an order of magnitude. *Fernando* [1991] also claims that Γ may depend on various factors, among others Pr, which is in agreement with our theoretically derived result, (7).

[17] By assuming $\boldsymbol{U} = \boldsymbol{U}(x_3)$, i.e., horizontally divergence-free flow, the second term on the right-hand side of (7) can be neglected. This yields a mixing efficiency only dependent on Pr. For atmospheric flows, (7) gives $\Gamma \sim 0.95$

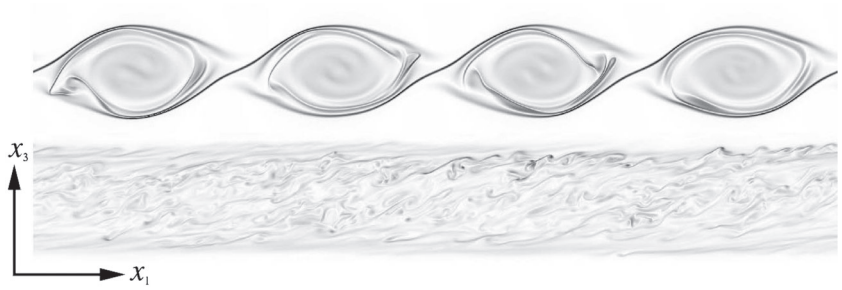

Figure 1. Contours of instantaneous vorticity magnitudes at (top) $t^* = 50$ and (bottom) $t^* = 227$. C.f. also Figures 2 and 3.

which is within the range shown in previous studies. Finally, it should be noted that the commonly used assumption of homogeneous turbulence has not been invoked in the present analysis.

2.2.3. New Dissipation Model

[18] Inspired by this discussion, the functional dependence of the viscous dissipation rate on mean temperature gradient and dissipation rate of temperature variance is further investigated. The motivation is that both the mean temperature gradient and the dissipation rate of temperature variance can be measured fairly accurately, which thus potentially provides a dissipation rate model applicable to full scale flows. This is true particularly in atmospheric flows, where Pr $\sim$ 1, implying that the scales of thermal dissipation is similar to those of viscous dissipation. By assuming horizontally divergence-free flow, the left-hand side of (6) vanishes and the proposed model takes the form

$$\varepsilon_{\mathrm{mod}} = -C_\varepsilon \frac{\varepsilon_\theta g_i \beta \mathrm{Pr}}{\partial_i \Theta}, \tag{8}$$

in which C_ε is an a priori unknown model coefficient. $C_\varepsilon = 3/2$ corresponds to locally isotropic turbulence. Generally, C_ε will depend on the flow characteristics. For oceanic flows, in which Pr $\sim$ 10, the scales of thermal dissipation are approximately an order of magnitude smaller than those of viscous dissipation [*Chung and Matheou*, 2012]. Equation (8) can in that case be rearranged to express ε_θ in terms of ε if desirable.

[19] For comparative purposes, the model advocated by *Weinstock* [1981], developed to account for stratification, is also included in the present study:

$$\varepsilon_{\mathrm{W}} = 0.4\langle u_3^2 \rangle N.$$

The isotropic formulation (see, e.g., *Thoroddsen and Van Atta* [1992] for derivation), where isotropic turbulence is assumed, is perhaps the most used and well-known dissipation model, requiring the measurement of only one (arbitrary) component of the fluctuating velocity gradient. Two variants of this model, based on different components of the fluctuating velocity gradient, will also be used for comparison:

$$\varepsilon_{\mathrm{iso1}} = 7.5\nu\langle(\partial_3 u_1)^2\rangle,$$
$$\varepsilon_{\mathrm{iso2}} = 7.5\nu\langle(\partial_1 u_3)^2\rangle.$$

2.3. Numerical Database

[20] In the DNS, gravity acts in the vertical direction, x_3. The domain is periodic in both horizontal (x_1 and x_2) directions, and symmetry conditions are imposed on the vertical boundaries. A third-order Runge-Kutta method is used to integrate in time, and the solver is pseudo-spectral in space. The domain size is $4\lambda \times 2\lambda \times 2\lambda$, where λ is the wavelength of the most unstable eigenmode of the Kelvin-Helmholtz instability. Further details can be found in *Werne et al.* [2005].

[21] The initial flow at $t^* = 0$, where $t^* = tU_0/H$ is dimensionless time, comprises a small perturbation superposed on a background velocity field $\tilde{\boldsymbol{u}} = [U_0 \tanh(x_3/H), 0, 0]$ and the temperature field $\tilde{\theta} = \alpha x_3$, where α is a constant coefficient. The parameters characterizing the initial flow fields are the Richardson number $Ri = g\beta\alpha H^2/U_0^2 = 0.05$, the Reynolds number $Re = U_0 H/\nu = 2500$, and $Pr = 1$. Here H and U_0 denote half the initial shear layer depth and the freestream velocity, respectively.

[22] The evolution of the flow field undergoes several stages (for a more detailed description, see, e.g., *Werne et al.* [2005], *Fritts et al.* [1996], and *Palmer et al.* [1996]). A shear layer instability develops with time, leading initially to Kelvin-Helmholtz billows (Figure 1, top) that become unstable, and subsequently develops into a fully turbulent shear layer. For the small scales, the imposition of the stably stratified background becomes significant at a later stage of the shear layer development in the simulation, which gradually suppresses the turbulence levels such that the flow field ultimately undergoes relaminarization. During the later stages (at which stratification starts to be important), the shear layer

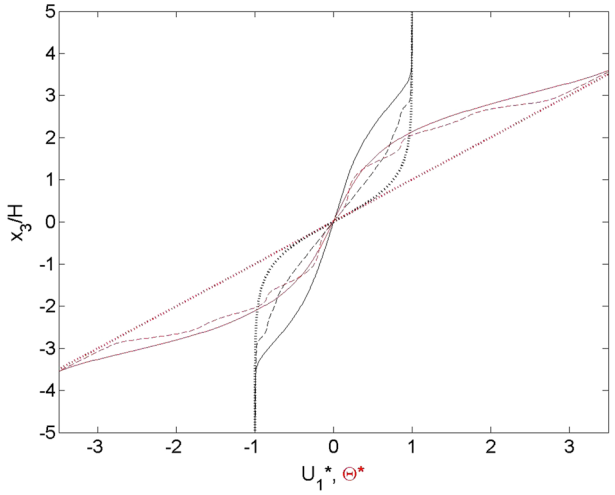

Figure 2. Nondimensional mean velocity, $U_1^* = U_1/U_0$, and mean temperature, $\Theta^* = \Theta/(\alpha H)$, profiles at $t^* = 0$ (·····), 50 (– – –), and 227 (——).

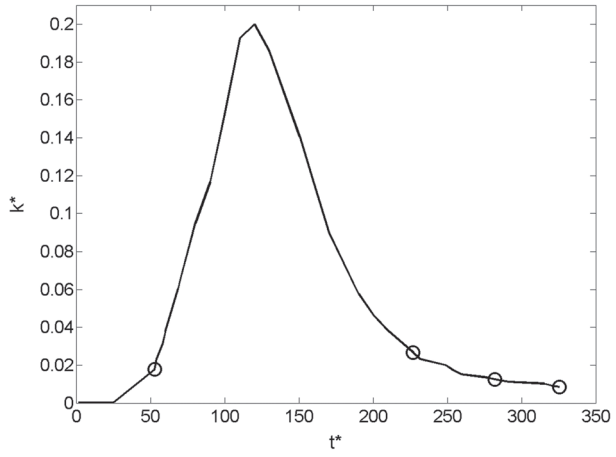

Figure 3. Nondimensional turbulence kinetic energy, $k^* = \int k \mathrm{d}x_3/(U_0^2 H)$, versus t^*. The symbols mark $t^* = 50$, 227, 282, and 325.

thickness becomes almost constant ($-3.5 < x_3 < 3.5$), and the flow field comes very close to being statistically homogeneous in the streamwise (x_1) direction. This occurs at $t^* \gtrsim 227$, cf. Figure 1 (bottom).

[23] In the present study, this particular stage of the flow evolution is in focus. Turbulence statistics are obtained by spatially averaging the flow field in both horizontal directions.

[24] Figure 2 shows the initial mean profiles of velocity and temperature, as well as the profiles for two later times, corresponding to the two time instances shown in Figure 1.

[25] The turbulence kinetic energy, $k = \frac{1}{2}\langle u_i u_i \rangle$, is shown on nondimensional form as a function of time in Figure 3. Here, the statistical correlations are obtained by spatially averaging in the horizontal directions. Since the flow field is statistically unsteady, time averaging is not justified. Despite similar turbulence kinetic energy levels around the times $t^* = 50$ and $t^* = 227$, the turbulence Reynolds number, $\mathrm{Re_T} = k^2/(\varepsilon\nu)$, varies greatly with time. This reflects the scale separation; early in the simulation, when the flow is essentially laminar, $\max\{\mathrm{Re_T}\} = 92.3$, whereas late in the simulation, $\max\{\mathrm{Re_T}\} = 555.6$. The maximum value of $\mathrm{Re_T} = 2706$ occurs at $t^* = 220$, and the maximum value of $\mathrm{Re_b} = 142$ occurs at $t^* = 110$. This buoyancy Reynolds number is below the critical value of 200, indicating a degree of anisotropy also at the small scales of the flow.

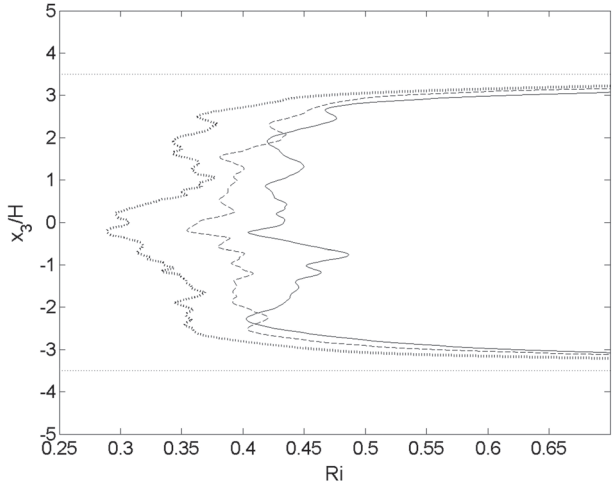

Figure 4. Local Richardson number at $t^* = 227$ (·····), 282 (– – –), and 325 (——). Layer edges are marked by horizontal dotted lines ($x_3/H = \pm 3.5$).

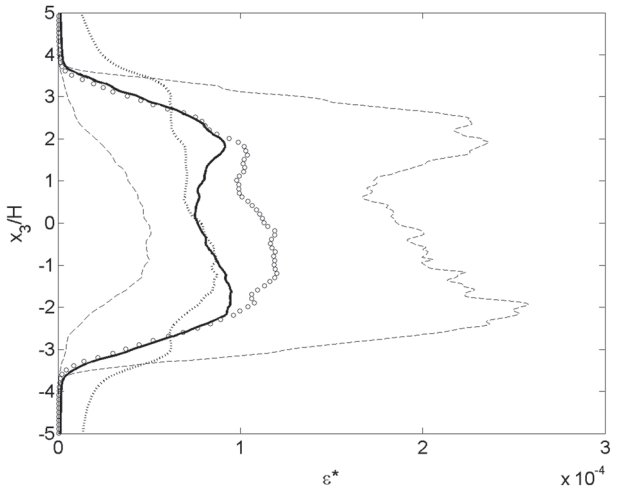

Figure 5. Nondimensional turbulence dissipation rate, $\varepsilon^* = \varepsilon H/U_0^3$, at $t^* = 227$; ∘ ∘ ∘ (DNS); —— (proposed model); ····· (Weinstock); – – – (isotropic models). $\min\{Ri\} = 0.29$.

[26] For $t^* \gtrsim 227$, stable stratification becomes dynamically important, which coincides with the time when nearly homogeneous turbulence develops. The turbulence dissipation rate is evaluated during this phase of the flow evolution. From time $t^* \gtrsim 227$, $\min\{\mathrm{Ri_{loc}}\} > 0.3$, where the local Richardson number is defined as $\mathrm{Ri_{loc}} = \beta g \partial_3 \Theta/(\partial_3 U_1)^2$.

[27] The local Richardson number at $t^* = 227$, 282, and 325 is shown in Figure 4. These three time instances correspond to the times at which the dissipation models are evaluated. The horizontal lines in Figure 4 mark the approximate edges of the shear layer.

3. Results and Discussion

[28] In light of the previous discussion, comparison of the newly proposed dissipation rate model to DNS results and other models will be restricted to $\mathrm{Ri_{loc}} > 0.3$. For such conditions, a suitable value of the empirical model coefficient is found to be $C_\varepsilon = 4.5$ (recall that $C_\varepsilon = 3/2$ corresponds to isotropic turbulence). This further implies that with the proposed model, the mixing efficiency $\Gamma = (C_\varepsilon \mathrm{Pr})^{-1} \approx 0.22$. Note that for other flows, the value of C_ε, and subsequently Γ, might differ.

[29] When using the isotropic formulation to estimate turbulence dissipation rate in an anisotropic field, it is not possible to know a priori which fluctuating velocity gradient component is the most appropriate to use. Systematic studies may indicate which components are best suited for certain kinds of flow, such as the results of *Smyth and Moum* [2000] related to stably stratified shear flow. Ideally, if the dissipative scales of the flow were isotropic, this choice would be arbitrary. Consequently, depending on the choice of component, the estimated dissipation rate can attain a range of values. To reflect this potential variation, two isotropic models that represent the extremes (maximum and minimum) of all the possible isotropic estimates are used. Hence, the esti-

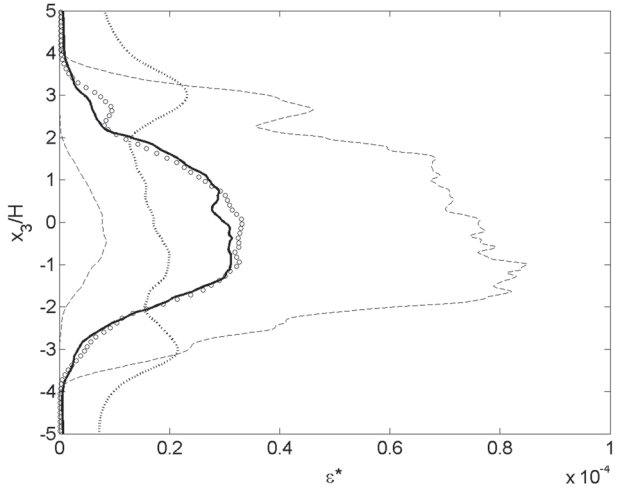

Figure 6. Nondimensional turbulence dissipation rate, $\varepsilon^* = \varepsilon H/U_0^3$, at $t^* = 282$; ∘ ∘ ∘ (DNS); —— (proposed model); ····· (Weinstock); – – – (isotropic models). min{Ri} = 0.35.

mated dissipation rate falls anywhere between $\varepsilon_{\text{iso1}}$ and $\varepsilon_{\text{iso2}}$, depending on the choice of velocity gradient component if the isotropic formulation is used.

[30] Figures 5–7 show the estimated and exact dissipation rates at $t^* = 227$, 282, and 325, respectively.

[31] At $t^* = 227$ (Figure 5), the proposed dissipation rate model is in good agreement with the DNS data, particularly at the edges of the turbulent layer. Near the centerline ($x_3/H = 0$) Weinstock's model is as close to the DNS value as the new model, but both models underpredict the dissipation rate slightly. Figure 4 shows that the local Richardson number is significantly lower close to the centerline than near the edges, indicating less stable flow in that region. This is most likely the reason why the proposed model is less accurate close to $x_3/H = 0$. The large range of possible outcomes from the isotropic formulation should also be noted; not surprisingly, the isotropic models seem unsuited for stably stratified flows in that they give such a wide range of results, thus also implying lack of isotropy, even at the dissipative scales.

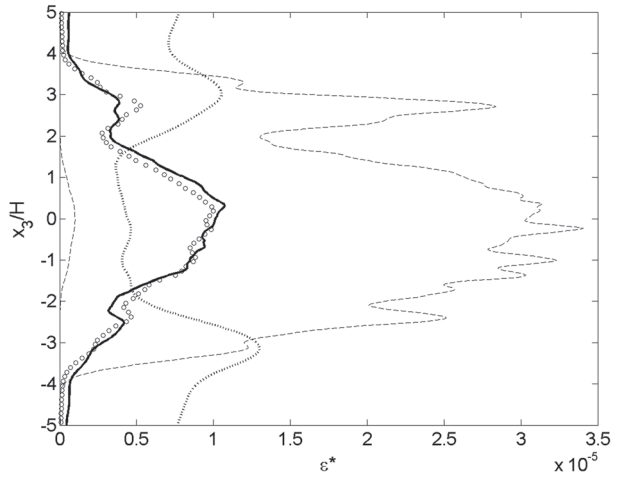

Figure 7. Nondimensional turbulence dissipation rate, $\varepsilon^* = \varepsilon H/U_0^3$, at $t^* = 325$; ∘ ∘ ∘ (DNS); —— (proposed model); ····· (Weinstock); – – – (isotropic models). min{Ri} = 0.40.

Table 1. Integrated Turbulence Dissipation Rate Across the Shear Layer, $\int_{-3.5}^{3.5} \varepsilon dx_3/U_0^3$

Time	DNS	Proposed Model	Weinstock	Isotropic
$t^* = 227$	0.024	0.0203	0.0196	0.0075 – 0.0519
$t^* = 282$	0.0047	0.0045	0.0045	0.0008 – 0.0140
$t^* = 325$	0.0014	0.0014	0.0017	0.0001 – 0.0057

[32] From Figures 6 and 7, in combination with Figure 4, there seems to be a tendency that the proposed dissipation rate model performs better as the level of stable stratification increases. At $t^* = 282$ and 325, the proposed model agrees remarkably well with the DNS results. In this case, Weinstock's model underpredicts the dissipation rate close to the center of the turbulent layer and exaggerates it near the layer edges. It should also be noted that the magnitude of the dissipation rate varies with an order of magnitude from $t^* = 227$ to $t^* = 325$.

[33] The results of Figures 5–7 are summarized in Table 1. Despite the disagreement locally, Weinstock's model does surprisingly well in estimating the total dissipation rate within the shear layer. The proposed model performs even better. At most (at $t^* = 227$), the deviation from the DNS data is 15%. By contrast, the isotropic estimates differ as much as 93% (at $t^* = 325$).

4. Concluding Remarks

[34] A new model for the turbulence dissipation rate in stably stratified turbulent flows has been derived and compared to DNS data as well as to two other types of models. Comparison with DNS data demonstrated that the proposed model performs very well for $\text{Ri}_{\text{loc}}0.3$. As opposed to most other algebraic models, the proposed model is functionally dependent on measurable quantities, thus making the model suitable also for use with experimental data.

[35] A further simplification of the model would be to replace the thermal dissipation rate with only one of its fluctuating temperature gradients. Based on the DNS data, the most appropriate choice would be to use $\langle(\partial_3\theta)^2\rangle$ which dominates the contribution to ε_θ. Such a modification would require recalibration of the model coefficient, C_ε, in (8).

[36] **Acknowledgments.** The authors are grateful to Joseph Werne for providing the DNS database, as well as valuable assistance. Magnus Drivdal is also acknowledged for fruitful discussions. This work was partly funded by Norwegian Research Council project 214881.

[37] The Editor thanks two anonymous reviewers for their assistance in evaluating this paper.

References

Batchelor, G. (1946), The theory of axisymmetric turbulence, *Proc. R. Soc. London, Ser.*, *186*(1007), 480–502.

Chung, D., and G. Matheou (2012), Direct numerical simulation of stationary homogeneous stratified sheared turbulence, *J. Fluid Mech.*, *696*(410), 434–467.

Fernando, H. J. (1991), Turbulent mixing in stratified fluids, *Annu. Rev. Fluid Mech.*, *23*(1), 455–493.

Fritts, D. C., T. L. Palmer, Ø. Andreassen, and I. Lei (1996), Evolution and breakdown of Kelvin–Helmholtz billows in stratified compressible flows. Part I: Comparison of two- and three-dimensional flows, *J. Atmos. Sci.*, *53*, 3173–3191.

Galperin, B., and S. Sukoriansky (2010), Geophysical flows with anisotropic turbulence and dispersive waves: Flows with stable stratification, *Ocean Dyn.*, *60*(5), 1319–1337.

George, W., and H. Hussein (1991), Locally axisymmetric turbulence, *J. Fluid Mech.*, *233*, 1–23.

Kolmogorov, A. (1941), The local structure of turbulence in incompressible viscous fluid for very large Reynolds' numbers, *Akad. Nauk SSSR Dokl.*, *30*, 301–305.

Limbacher, J. (2010), A comparison of methods used to estimate the turbulent kinetic energy dissipation rate in the atmospheric surface layer, PhD thesis, Penn. State Univ., University Park.

McIntyre, M. E. (1989), On dynamics and transport near the polar mesopause in summer, *J. Geophys. Res.*, *94*(D12), 14,617–14,628.

Palmer, T. L., D. C. Fritts, and Ø. Andreassen (1996), Evolution and breakdown of Kelvin–Helmholtz billows in stratified compressible flows. Part II: Instability structure, evolution, and energetics, *J. Atmos. Sci.*, *53*, 3192–3212.

Reif, B., and Ø. Andreassen (2003), On local isotropy in stratified homogeneous turbulence, *SIAM J. Appl. Math.*, *64*(1), 309–321.

Smyth, W., and J. Moum (2000), Anistropy of turbulence in stably stratified mixing layers, *Phys. Fluids*, *12*, 1343–1362.

Taylor, G. (1935), Statistical theory of turbulence, *Proc. R. Soc. London, Ser.*, *151*(873), 421–444.

Thoroddsen, S., and C. Van Atta (1992), The influence of stable stratification on small-scale anisotropy and dissipation in turbulence, *J. Geophys. Res.*, *97*(C3), 3647–3658.

Weinstock, J. (1981), Energy dissipation rates of turbulence in the stable free atmosphere, *J. Atmos. Sci.*, *38*, 880–880.

Werne, J., T. Lund, and D. Fritts (2005), CAP Phase II Simulations for the Air Force HEL-JTO Project: Atmospheric turbulence simulations on NAVO's 3000-Processor IBM P4+ and ARL's 2000-Processor Intel Xeon EM64T Cluster, in *Users Group Conference, 2005*, edited by D. E. Post, pp. 100–111, Inst. of Electr. and Electron. Eng., Los Alamitos, CA, U.S.A.

Wyngaard, J. (2010), *Turbulence in the Atmosphere*, Cambridge Univ. Press, Cambridge, UK.

Xu, D., and J. Chen (2012), Accurate estimate of turbulent dissipation rate using PIV data, *Exp. Thermal Fluid Sci.*, *44*, 662–672.

Yamazaki, H., and T. Osborn (1990), Dissipation estimates for stratified turbulence, *J. Geophys. Res.*, *95*(C6), 9739–9744.